

Interfacial fluid flow for systems with anisotropic roughness

B.N.J. Persson^{1,2}

¹*PGI-1, FZ Jülich, Germany, EU*

²*MultiscaleConsulting, Wolfshovener str 2, 52428 Jülich, Germany*

I discuss fluid flow at the interface between solids with anisotropic roughness. I show that for randomly rough surfaces with anisotropic roughness, the contact area percolate at the same relative contact area as for isotropic roughness, and that the Bruggeman effective medium theory and the critical junction theory give nearly the same results for the fluid flow conductivity. This shows that, in most cases, the surface roughness observed at high magnification is irrelevant for fluid flow problems such as the leakage of static seals, and fluid squeeze-out.

1. Introduction

Fluid flow at the interface between elastic solids is a complicated topic, in general involving elastic deformations, complex fluid rheology and interfacial fluid slip[1]. In particular, the influence of the surface roughness on the fluid flow dynamics is a highly complex topic. However, if there is a separation of length scales the problem can be simplified: if R denote the (smallest) macroscopic radius of curvature of the (undeformed) surfaces in the nominal contact region, e.g., the radius of a ball, and if $R \gg \lambda_0$, where λ_0 is the longest (relevant) surface roughness component, then it is possible to eliminate (integrate out) the surface roughness and obtain effective fluid flow equations involving solid bodies with smooth surfaces (no roughness). The effective fluid flow equations depend on quantities determined by the surface roughness, usually denoted fluid flow and friction factors (there are two fluid flow factors and three friction factors). These factors depend on the average surface separation \bar{u} , which will vary throughout the nominal contact region; \bar{u} is the local interfacial surface separation $u(x, y)$ averaged over the surface roughness[2, 3]. In several publications it has been shown how to calculate the fluid flow factors, which enter in the (modified) Reynolds equation, and the friction factors, which enters in the expression for the shear stress acting on the solids[1, 4–10].

Here we consider the simplest fluid flow problems, which include the leakage of static seals[11, 12] and the squeeze-out of fluids[13] between elastic solids. For these applications the roughness enter only via one function, namely the pressure flow factor $\phi_p(\bar{u})$ (in general a 2×2 tensor) or, equivalently, the (effective) fluid flow conductivity σ_{eff} defined

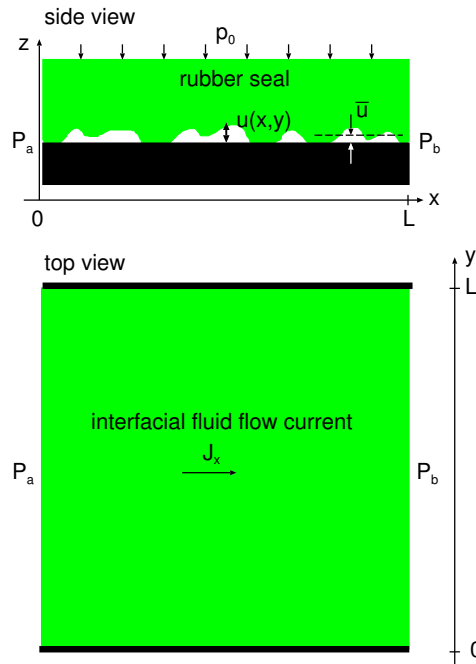


FIG. 1: A square block $L \times L$ rubber seal (green) with surface roughness squeezed with the uniform pressure p_0 against a flat rigid countersurface. A fluid pressure difference $\Delta P = P_a - P_b > 0$ occur between the two sides $x = 0$ and $x = L$. We assume no fluid leakage in the direction orthogonal to the x -axis i.e. two ends $y = 0$ and $y = L$ are blocked.

by the equation

$$\bar{\mathbf{J}} = -\sigma_{\text{eff}} \nabla \bar{p}$$

where $\bar{p} = \langle p(x, y) \rangle$ is the fluid pressure and $\bar{\mathbf{J}} = \langle \mathbf{J}(x, y) \rangle$ the two-dimensional (2D) fluid flow current, both averaged over the surface roughness (ensemble averaging). The flow conductivity σ_{eff} is a 2×2 matrix (tensor).

As an example, consider a seal consisting of a rubber block with square cross section $L \times L$, with surface roughness on length scales much smaller than L , squeezed against a flat surface (see Fig. 1). Assume that high pressure fluid occur for $x < 0$ and low pressure fluid for $x > L$ (pressure difference $\Delta P = P_a - P_b > 0$). In this case for the choosed coordinate system σ_{eff} is a diagonal matrix:

$$\sigma_{\text{eff}} = \begin{pmatrix} \sigma_x & 0 \\ 0 & \sigma_y \end{pmatrix}$$

with $\sigma_y = 0$. The pressure gradient $\nabla \bar{p}$ is along the x -axis and $d\bar{p}/dx = -\Delta P/L$. Thus, the fluid leakage rate (volume per unit time) becomes

$$\dot{Q} = L J_x = L \sigma_x \Delta P / L = \sigma_x \Delta P$$

From the fluid flow conductivity one can calculate the pressure flow factor

$$\phi_p = 12\eta \bar{u}^{-3} \sigma_{\text{eff}}$$

For two parallel surfaces without roughness one has the flow conductivity (Poiseuille flow):

$$\sigma_0 = \frac{u_0^3}{12\eta},$$

where u_0 is the surface separation. For a system with surface roughness it is sometimes convenient to define a separation u_c , which depends on the average surface separation \bar{u} , so that

$$\sigma_{\text{eff}} = \frac{u_c^3}{12\eta}$$

Thus the pressure flow factor

$$\phi_p = \left(\frac{u_c}{\bar{u}} \right)^3$$

In this paper I discuss fluid flow at the interface between solids with anisotropic roughness. I show that for randomly rough surfaces with anisotropic roughness, the contact area percolate at the same relative contact area as for isotropic roughness. I also show that, unless the applied pressure is very small, the Bruggeman effective medium theory and the critical junction theory give nearly the same results for the fluid flow conductivity (and the fluid pressure flow factor). This shows that for applications involves only the flow conductivity (or, equivalently, the pressure flow factor), such as the leakage of static seals and fluid squeeze-out, in most cases the (short wavelength) surface roughness observed at high magnification is irrelevant.

2. Qualitative discussion

The theory of fluid flow discussed in this paper is based on the Bruggeman effective medium theory. This theory is for an infinite-sized system but real applications and computer simulations involves systems of finite sizes. Finite size effects may in some cases be important, in particular for system with strongly anisotropic roughness such as surfaces grinded in one direction, and for systems with small nominal contact area.

Consider the contact between two elastic solids with random surface roughness. One way to (mathematically) produce systems with anisotropic roughness is to start with a surface with isotropic roughness, say a square area of size $L \times L$, and stretch the surface in the x -direction be a factor $\gamma^{1/2}$ and contract it in the y -direction by a factor $\gamma^{-1/2}$, as indicated in Fig. 2(b). This will map a circle on an ellipse (with the same surface area) where the ratio between the ellipse axis in the x - and y -directions is gives by γ (Peklenik number[14]).

To get a square unit surface we extend the surface in the y -direction with similar rectangular units (but other realizations) as in Fig. 2(b), see Fig. 2(c). If a surface region, with the same size $L \times L$ as the original surface, is

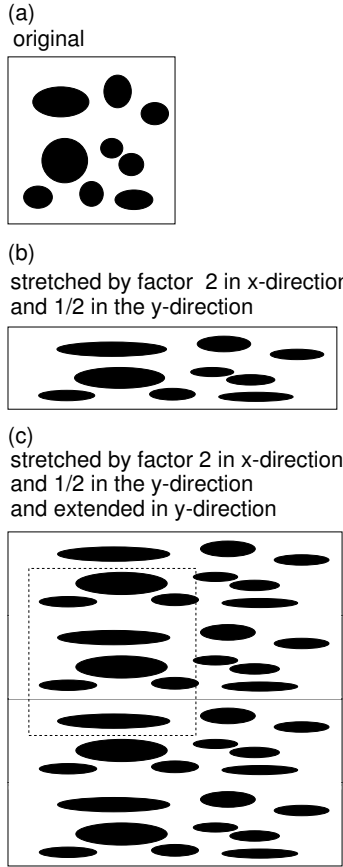


FIG. 2: (a) Asperity contact regions (black) for a system with random roughness with isotropic statistical properties, and (b), (c) for a system obtained by stretching by a factor of 2 in the x -direction and 1/2 in the y -direction. This transformation conserve the area and result in anisotropic roughness with $\gamma = 4$. For a system of finite size, if the system size is fixed [compare (a) with the dashed square in (c)] the contact area percolation threshold depends on the stretching factor γ , but for an infinite system the percolation threshold does not depend on γ .

cut-out of the surface in Fig. 2(c), the contact area may percolate in the x -direction (see dashed square in Fig. 2(c)) even if the contact area did not percolate for the original surface. *However, for the infinite system the stretching cannot change the percolation threshold.* This is clear since a flow channel which is closed before stretching remain closed after stretching, and a flow channel which is open before stretching will remain open after stretching. For a system with isotropic roughness the Bruggeman theory predict that the contact area percolate when $A/A_0 = 0.5$, and the same is true for a surface with anisotropic roughness (see Sec.5).

In Ref. [15] I presented an approximate formula for the fluid flow conductivity which interpolate between the Bruggeman effective medium theory result for isotropic roughness, and the known limit for the fluid flow conductivity for the case of strongly anisotropic roughness. The expression for the flow conductivity σ_x proposed in Ref. [15] is

$$\frac{1}{\sigma_x} = \left\langle \frac{1 + \gamma}{\sigma + \gamma \sigma_x} \right\rangle \quad (1)$$

where $\sigma = u^3/(12\eta)$, where η is the fluid viscosity and $u = u(\mathbf{x})$ the interfacial separation at the point $\mathbf{x} = (x, y)$. The $\langle \dots \rangle$ stands for ensemble averaging, or averaging over the probability distribution $P(u)$ of interfacial separations. For $\gamma = 1$ this equation reduces to the standard Bruggeman equation for isotropic roughness, while for $\gamma \rightarrow 0$ it gives $\sigma_x = \langle \sigma^{-1} \rangle^{-1}$ and for $\gamma \rightarrow \infty$ it gives $\sigma_x = \langle \sigma \rangle$. Both these limits are exact results as is easy to show directly from the Reynolds equation for thin film fluid flow. Nevertheless, for an infinite system (1) gives the wrong percolation condition (see below).

The flow conductivity in the y -direction is obtained from (1) by replacing γ with $1/\gamma$:

$$\frac{1}{\sigma_y} = \left\langle \frac{1 + (1/\gamma)}{\sigma + (1/\gamma)\sigma_y} \right\rangle \quad (2)$$

We can write the probability distribution of interfacial separation as[16, 17]

$$P(u) = \frac{A}{A_0} \delta(u) + P_c(u) \quad (3)$$

where $P_c(u)$ is the (continuous) part of the distribution where $u > 0$. Thus we get

$$\frac{1}{\sigma_x} = \frac{1+\gamma}{\sigma_x \gamma} \frac{A}{A_0} + \left\langle \frac{1+\gamma}{\sigma + \gamma \sigma_x} \right\rangle_c \quad (4)$$

When the contact area percolate no fluid flow is possible from one side to the other side of the studied unit, so that $\sigma_x \rightarrow 0$. When $\sigma_x \rightarrow 0$ using (4) gives

$$1 = \frac{1+\gamma}{\gamma} \frac{A}{A_0}$$

or $A/A_0 = \gamma/(1+\gamma)$. However, for an infinite system this result is incorrect and the relative contact area A/A_0 at the point where the contact area percolate does in fact not depend on γ .

Computer simulations of contact mechanics are always for finite-sized systems. In this case it has been observed that when $\gamma > 1$ the contact area percolate for a smaller relative contact area A/A_0 then when $\gamma = 1$. Similarly, for $\gamma < 1$ the contact area percolate for a larger A/A_0 then when $\gamma = 1$, and in one study the results was rather accurately described by the formula $A/A_0 = \gamma/(1+\gamma)$. These results are intuitively clear, but the simulation results depend on the system size, and is hence non-universal.

The Bruggeman effective medium theory gives flow conductivities of the form (1) and (2), but with γ replaced by $\gamma^* = \gamma(\sigma_y/\sigma_x)^{1/2}$ (see Sec. 4). For this case the percolation threshold occur when $A/A_0 = 0.5$ independent of γ (see Sec. 5).

3 Tripp number

The most important property characterizing a rough surface is the surface roughness power spectrum $C(\mathbf{q})$. If $z = h(\mathbf{x})$ is the height coordinate at the point $\mathbf{x} = (x, y)$ then the two-dimensional (2D) power spectrum $C(\mathbf{q}) = C(q_x, q_y)$ is given by

$$C(\mathbf{q}) = \frac{1}{(2\pi)^2} \int d^2x \langle h(\mathbf{x})h(\mathbf{0}) \rangle e^{i\mathbf{q}\cdot\mathbf{x}} \quad (5)$$

where $\langle \dots \rangle$ stands for ensemble averaging. For a surface with isotropic statistical properties, $C(\mathbf{q})$ depends only on the magnitude $q = |\mathbf{q}|$ of the 2D wave vector \mathbf{q} . For surfaces with anisotropic statistical properties the Tripp number[9] $\gamma(q)$ is very important as it determines the influence of the surface roughness anisotropy on interfacial fluid flow[9, 18]. The Tripp number depends on the length scale considered, i.e., it is a function of the wavenumber q , and is defined as follows[18]. We introduce polar coordinates $\mathbf{q} = q(\cos\phi, \sin\phi)$ and define the matrix

$$D(q) = \frac{\int_0^{2\pi} d\phi C(\mathbf{q})\mathbf{q}\mathbf{q}/q^2}{\int_0^{2\pi} d\phi C(\mathbf{q})} \quad (6)$$

Note that $D(q)$ is a symmetric matrix and can be diagonalized by an orthogonal transformation. We denote the diagonal elements by $1/(1+\gamma)$ and $\gamma/(1+\gamma)$ where $\gamma = \gamma(q)$ is the Tripp number, which depends on the wavenumber q . If $C(\mathbf{q})$ only depend on the magnitude of the wavevector then $D_{ij}(q) = \delta_{ij}/2$, so that $\gamma = 1$ for roughness with isotropic statistical properties.

One can also define the average Tripp number using

$$D = \frac{\int d^2q C(\mathbf{q})\mathbf{q}\mathbf{q}/q^2}{\int d^2q C(\mathbf{q})} \quad (7)$$

Let us study

$$I = \int d^2q C(\mathbf{q}) \frac{\mathbf{q}\mathbf{q}}{q^2}$$

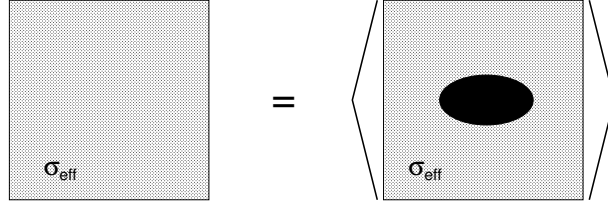


FIG. 3: In the effective medium approach a system with anisotropic roughness is replaced by an effective system with the (constant) flow conductivity σ_{eff} . The effective flow conductivity is determined as follows: An elliptic region with the constant surface separation u is embedded in the effective medium. The flow current $\mathbf{J}_u(x, y)$ for this system depends on the surface separation u in the elliptic region. The effective conductivity is determined by the condition that \mathbf{J}_u averaged over the probability distribution of surface separations $P(u)$ is equal to the flow current obtained using the effective medium everywhere.

for a particular case. Assume that $f(x, y) = f(r)$ only depend on the magnitude of the coordinate \mathbf{x} and consider the function $f(x/a_x, y/a_y)$. If $f(r) = 0$ is a circle then $f(x/a_x, y/a_y) = 0$ is an ellipse. In wavevector space we get the function $g(q_x a_x, q_y a_y)$. Assume that $C(\mathbf{q}) = g(q_x a_x, q_y a_y)$ with $g(q_x, q_y) = g(q)$. Writing $q'_x = q_x a_x$, $q'_y = q_y a_y$ we get

$$I = \frac{1}{a_x a_y} \int d^2 q' g(q') \frac{1}{(q'_x/a_x)^2 + (q'_y/a_y)^2} \begin{pmatrix} (q'_x/a_x)^2 & q'_x q'_y / (a_x a_y) \\ q'_x q'_y / (a_x a_y) & (q'_y/a_y)^2 \end{pmatrix}$$

In polar coordinates

$$q'_x = q' \cos \phi, \quad q'_y = q' \sin \phi$$

we get

$$I = \frac{1}{a_x a_y} \int d^2 q' g(q') \frac{1}{a_x^{-2} \cos^2 \phi + a_y^{-2} \sin^2 \phi} \begin{pmatrix} a_x^{-2} \cos^2 \phi & (a_x a_y)^{-1} \cos \phi \sin \phi \\ (a_x a_y)^{-1} \cos \phi \sin \phi & a_y^{-2} \sin^2 \phi \end{pmatrix}$$

or

$$I = \frac{1}{a_x a_y} \int d^2 q' g(q') \frac{1}{\cos^2 \phi + \gamma^2 \sin^2 \phi} \begin{pmatrix} \cos^2 \phi & 0 \\ 0 & \gamma^2 \sin^2 \phi \end{pmatrix} \quad (8)$$

Let us denote $a_x/a_y = \gamma$ which we refer to as the Tripp number. Since $g(q')$ only depend on the magnitude of \mathbf{q}' we can write (8) as

$$I = \frac{1}{a_x a_y} \int d^2 q' g(q') \frac{1}{2\pi} \int d\phi \frac{1}{\cos^2 \phi + \gamma^2 \sin^2 \phi} \begin{pmatrix} \cos^2 \phi & 0 \\ 0 & \gamma^2 \sin^2 \phi \end{pmatrix}$$

Finally using that

$$\frac{1}{a_x a_y} \int d^2 q' g(q') = \int d^2 q g(q_x a_x, q_y a_y) = \int d^2 q C(\mathbf{q})$$

we get

$$D = \frac{1}{2\pi} \int d\phi \frac{1}{\cos^2 \phi + \gamma^2 \sin^2 \phi} \begin{pmatrix} \cos^2 \phi & 0 \\ 0 & \gamma^2 \sin^2 \phi \end{pmatrix}$$

The integral over ϕ is easy to perform (see Appendix A) giving

$$D = \frac{1}{1 + \gamma} \begin{pmatrix} 1 & 0 \\ 0 & \gamma \end{pmatrix} \quad (9)$$

4 Bruggeman effective medium theory for fluid flow

Effective medium theories are simple, but very useful and often accurate methods to describe some properties of inhomogeneous materials. The effective medium approach assumes that the material is randomly disordered at

length scales much shorter than the the length scale of interest. Typical applications of effective medium theories are the optical properties of inhomogeneous materials, and the electric or fluid transport in inhomogeneous materials. There are several different (but related) effective medium theories, e.g. the coherent potential approximation or the Bruggeman effective medium approximation[19–26]. In earlier publications we have shown how the leakage of seals can be accurately described using the Bruggeman effective medium theory for systems with random but isotropic surface roughness[12].

The fluid flow current

$$\mathbf{J} = -\sigma \nabla p \quad (10)$$

where

$$\sigma = \frac{u^3}{12\eta} \quad (11)$$

where $u(\mathbf{x})$ is the interfacial separation at the point \mathbf{x} and η the fluid viscosity. Conservation of mass

$$\nabla \cdot \mathbf{J} = 0 \quad (12)$$

We will replace the inhomogeneous system with a homogeneous system with the average interfacial separation $\bar{u}(\mathbf{x})$ which can be treated as locally a constant. The average flow current

$$\bar{\mathbf{J}} = -\sigma_{\text{eff}} \nabla \bar{p} \quad (13)$$

The flow conductivity σ_{eff} in the Bruggeman effective medium approach is determined as indicated in Fig. 3. That is, in the effective medium approach a system with anisotropic roughness is replaced by an effective system with the (constant) flow conductivity σ_{eff} . The effective flow conductivity is determined as follows: An elliptic region with the constant surface separation u is embedded in the effective medium. The flow current $\mathbf{J}_u(x, y)$ for this system depends on the surface separation u in the elliptic region. The effective conductivity is determined by the condition that \mathbf{J}_u averaged over the probability distribution of surface separations $P(u)$ is equal to the flow current obtained using the effective medium everywhere.

The treatment which follows is similar to those presented in Ref. [20] and [21]. Let us write

$$\mathbf{J}_u = -\sigma \nabla p \quad \text{inside the elliptic region} \quad (14)$$

$$\mathbf{J}_u = -\sigma_{\text{eff}} \nabla p \quad \text{outside the elliptic region} \quad (15)$$

Thus if we define

$$\mathbf{J}_u = -\sigma_{\text{eff}} \nabla p + \mathbf{J}_1 \quad (16)$$

then $\mathbf{J}_1 = \mathbf{0}$ outside the elliptic region. Using (12) we get

$$\nabla \cdot \sigma_{\text{eff}} \nabla p = \nabla \cdot \mathbf{J}_1 = \int d^2 x' \delta(\mathbf{x} - \mathbf{x}') \nabla \cdot \mathbf{J}_1(\mathbf{x}') \quad (17)$$

If we define

$$\nabla \cdot \sigma_{\text{eff}} \nabla G(\mathbf{x} - \mathbf{x}') = \delta(\mathbf{x} - \mathbf{x}') \quad (18)$$

we can write

$$\nabla \cdot \left[\sigma_{\text{eff}} \left(\nabla p - \int d^2 x' \nabla G(\mathbf{x} - \mathbf{x}') \nabla' \cdot \mathbf{J}_1(\mathbf{x}') \right) \right] = 0$$

This equation is satisfied by

$$\nabla p - \int d^2 x' \nabla G(\mathbf{x} - \mathbf{x}') \nabla' \cdot \mathbf{J}_1(\mathbf{x}') = \nabla p^o$$

where ∇p^o is a constant vector. Thus

$$\nabla p = \nabla p^o + \int d^2 x' \nabla \nabla G(\mathbf{x} - \mathbf{x}') \cdot \mathbf{J}_1(\mathbf{x}') \quad (19)$$

where we have performed a partial integration and used that $\mathbf{J}_1(\mathbf{x})$ vanish outside the elliptic region.

The problem above involves equations very similar to those in electrostatics (see Appendix B). From electrostatics we know that if an elliptic (homogeneous) body is embedded in a (homogeneous) dielectric media, in an applied electric field the electric polarization in the inclusion is uniform. In the present case this imply that \mathbf{J}_1 is constant in the elliptic region where the interfacial separation equals u (a constant). Since \mathbf{J}_1 vanish outside the elliptic region, if we define $f(\mathbf{x}) = 1$ inside the elliptic region and $f(\mathbf{x}) = 0$ outside, we can write (19) as

$$\nabla p = \nabla p^o + Q \cdot \mathbf{J}_1 \quad (20)$$

where the matrix

$$Q = \int d^2x f(\mathbf{x}) \nabla \nabla G(\mathbf{x}) \quad (21)$$

where the integral is over the whole xy -plane. Since $\mathbf{J}_u = -\sigma \nabla p$ inside the elliptic region (see (14)) from (16) we get

$$\mathbf{J}_1 = (\sigma_{\text{eff}} - \sigma) \nabla p \quad (22)$$

Substituting this in (20) gives

$$\nabla p = \nabla p^o + Q \cdot (\sigma_{\text{eff}} - \sigma) \nabla p$$

or

$$[1 - Q \cdot (\sigma_{\text{eff}} - \sigma)] \nabla p = \nabla p^o$$

or

$$\nabla p = [1 - Q \cdot (\sigma_{\text{eff}} - \sigma)]^{-1} \nabla p^o \quad (23)$$

Using (22) and (23) we get

$$\mathbf{J}_1 = (\sigma_{\text{eff}} - \sigma) \nabla p = (\sigma_{\text{eff}} - \sigma) [1 - Q \cdot (\sigma_{\text{eff}} - \sigma)]^{-1} \nabla p^o$$

We demand that the average of \mathbf{J}_1 vanish which gives

$$\langle \mathbf{J}_1 \rangle = \langle (\sigma_{\text{eff}} - \sigma) [1 - Q \cdot (\sigma_{\text{eff}} - \sigma)]^{-1} \rangle \nabla p^o = 0$$

Since ∇p^o is an arbitrary constant vector we get

$$\langle (\sigma_{\text{eff}} - \sigma) [1 - Q \cdot (\sigma_{\text{eff}} - \sigma)]^{-1} \rangle = 0 \quad (24)$$

Since Q is a diagonal matrix (see below) with components Q_{11} and Q_{22} , the matrix $M = [1 - Q \cdot (\sigma_{\text{eff}} - \sigma)]$ is also diagonal with the elements

$$M_{11} = 1 - Q_{11}(\sigma_x - \sigma)$$

and

$$M_{22} = 1 - Q_{22}(\sigma_y - \sigma)$$

Thus we get from (24):

$$\left\langle \frac{\sigma_x - \sigma}{1 - Q_{11}(\sigma_x - \sigma)} \right\rangle = 0 \quad (25)$$

$$\left\langle \frac{\sigma_y - \sigma}{1 - Q_{22}(\sigma_y - \sigma)} \right\rangle = 0 \quad (26)$$

The Fourier transform of (18) gives

$$-\mathbf{q} \cdot \sigma_{\text{eff}} \mathbf{q} G(\mathbf{q}) = \frac{1}{(2\pi)^2}$$

or

$$G(\mathbf{q}) = -\frac{1}{(2\pi)^2} \frac{1}{\sigma_x q_x^2 + \sigma_y q_y^2} \quad (27)$$

and (20) gives

$$\begin{aligned} Q &= \int d^2x \int d^2q \int d^2q' f(\mathbf{q}')(-\mathbf{q}\mathbf{q})G(\mathbf{q})e^{i(\mathbf{q}+\mathbf{q}')\cdot\mathbf{x}} \\ &= (2\pi)^2 \int d^2q f(\mathbf{q})(-\mathbf{q}\mathbf{q})G(\mathbf{q}) \end{aligned} \quad (28)$$

Using (27) and (28) and $q'_x = q_x a_x$, $q'_y = q_y a_y$ and using that $f(\mathbf{q}) = f(q')$ we get

$$Q = \frac{1}{a_x a_y} \int d^2q' f(q') \frac{1}{\sigma_x (q'_x/a_x)^2 + \sigma_y (q'_y/a_y)^2} \begin{pmatrix} (q'_x/a_x)^2 & q'_x q'_y / (a_x a_y) \\ q'_x q'_y / (a_x a_y) & (q'_y/a_y)^2 \end{pmatrix}$$

or

$$Q = \frac{1}{a_x a_y} \int d^2q' f(q') \frac{1}{2\pi} \int d\phi \frac{1}{\sigma_x a_x^{-2} \cos^2 \phi + \sigma_y a_y^{-2} \sin^2 \phi} \begin{pmatrix} a_x^{-2} \cos^2 \phi & (a_x a_y)^{-1} \cos \phi \sin \phi \\ (a_x a_y)^{-1} \cos \phi \sin \phi & a_y^{-2} \sin^2 \phi \end{pmatrix}$$

Using that

$$\frac{1}{a_x a_y} \int d^2q' f(q') = \int d^2q f(\mathbf{q}) = f(\mathbf{x} = \mathbf{0}) = 1$$

we get

$$\begin{aligned} Q &= \frac{1}{2\pi} \int d\phi \frac{1}{\sigma_x a_x^{-2} \cos^2 \phi + \sigma_y a_y^{-2} \sin^2 \phi} \begin{pmatrix} a_x^{-2} \cos^2 \phi & (a_x a_y)^{-1} \cos \phi \sin \phi \\ (a_x a_y)^{-1} \cos \phi \sin \phi & a_y^{-2} \sin^2 \phi \end{pmatrix} \\ &= \frac{1}{2\pi \sigma_x} \int d\phi \frac{1}{\cos^2 \phi + \gamma^2 (\sigma_y / \sigma_x) \sin^2 \phi} \begin{pmatrix} \cos^2 \phi & 0 \\ 0 & \gamma^2 \sin^2 \phi \end{pmatrix} \end{aligned}$$

Using (A1) and (A2) this gives

$$Q_{11} = \frac{1}{\sigma_x} \frac{1}{1 + \gamma (\sigma_y / \sigma_x)^{1/2}} \quad (29)$$

$$Q_{22} = \frac{1}{\sigma_y} \frac{\gamma (\sigma_y / \sigma_x)^{1/2}}{1 + \gamma (\sigma_y / \sigma_x)^{1/2}} \quad (30)$$

Substituting (29) in (25) and (30) in (26) gives

$$\frac{1}{\sigma_x} = \left\langle \frac{1 + \gamma^*}{\sigma + \gamma^* \sigma_x} \right\rangle \quad (31)$$

$$\frac{1}{\sigma_y} = \left\langle \frac{1 + (1/\gamma^*)}{\sigma + (1/\gamma^*) \sigma_y} \right\rangle \quad (32)$$

where $\gamma^* = \gamma (\sigma_y / \sigma_x)^{1/2}$.

5 Limiting cases

Consider first the case when $\gamma^* \rightarrow \infty$. In this case from (31) we get $\sigma_x = \langle \sigma \rangle$ and from (32) $\sigma_y = \langle \sigma^{-1} \rangle^{-1}$. Note that

$$\gamma^* = \gamma \left(\frac{\sigma_y}{\sigma_x} \right)^{1/2} = \frac{\gamma}{(\langle \sigma \rangle \langle \sigma^{-1} \rangle)^{1/2}}$$

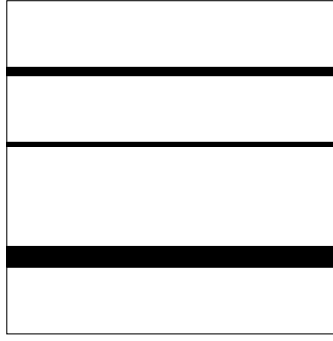


FIG. 4: Example of area of real contact (black) as $\gamma \rightarrow \infty$.

Thus if $\gamma \rightarrow \infty$ it follows that $\gamma^* \rightarrow \infty$.

Note that when $\gamma^* \rightarrow \infty$, if the area of real contact $A > 0$ we get $\langle u^{-1} \rangle^{-1} = 0$, so that $\sigma_y = 0$ and no fluid can flow in the y -direction. This result is clear from a physical point of view since strips of contact will extend between the two edges of the system in the x -direction as indicated in Fig. 4 and no fluid flow is possible. The results for σ_x and σ_y when $\gamma \rightarrow \infty$ (or $\gamma \rightarrow 0$) are well known and can be easily obtained directly from the Reynold thin-film fluid flow equation with $u(x, y)$ only depending on y (or x).

Next, let us consider the case when we increase the nominal contact pressure so we approach the limit when the contact area percolate. When the contact area percolate no fluid flow is possible from one side to the other side of the studied unit, so that $\sigma_x \rightarrow 0$. We can write the probability distribution of interfacial separation as [16, 17]

$$P(u) = \frac{A}{A_0} \delta(u) + P_c(u)$$

where $P_c(u)$ is the part of the distribution where $u > 0$. Thus we get

$$\frac{1}{\sigma_x} = \frac{1 + \gamma^*}{\sigma_x \gamma^*} \frac{A}{A_0} + \left\langle \frac{1 + \gamma^*}{\sigma + \gamma^* \sigma_x} \right\rangle_c \quad (33)$$

$$\frac{1}{\sigma_y} = \frac{1 + \gamma^*}{\sigma_y} \frac{A}{A_0} + \left\langle \frac{1 + (1/\gamma^*)}{\sigma + (1/\gamma^*) \sigma_y} \right\rangle_c \quad (34)$$

where $\langle \dots \rangle_c$ stands for averaging using $P_c(u)$ i.e., over the non-contact surface area $A_0 - A$. From (33) as $\sigma_x \rightarrow 0$ we get

$$1 = \frac{1 + \gamma^*}{\gamma^*} \frac{A}{A_0} \quad (35)$$

We will now show that $\sigma_x \rightarrow 0$ imply $\sigma_y \rightarrow 0$ i.e. the contact area percolate in both the x and y -directions at the same time. To prove this, assume that this is not the case so σ_y remains non-zero as $\sigma_x \rightarrow 0$. It then follows that $\gamma^* = \gamma(\sigma_y/\sigma_x)^{1/2} \rightarrow \infty$ as $\sigma_x \rightarrow 0$. In this case (35) gives $A/A_0 = 1$. This result is incorrect because we know that the contact area when $\gamma = 1$ percolate when $A/A_0 = 0.5$. Thus $\sigma_x \rightarrow 0$ imply $\sigma_y \rightarrow 0$ and from (34) we get

$$1 = (1 + \gamma^*) \frac{A}{A_0} \quad (36)$$

Using (35) and (36) gives $\gamma^* = 1$ and $A/A_0 = 1/2$. Using $\gamma^* = \gamma(\sigma_y/\sigma_x)^{1/2}$ and $\gamma^* = 1$ we get $\sigma_x = \gamma^2 \sigma_y$, which holds as $\sigma_x \rightarrow 0$.

Finally, let us consider the case when the separation $u(\mathbf{x}) = \bar{u} + \delta u(\mathbf{x})$ where \bar{u} is the average separation and $\delta u/\bar{u} \ll 1$. This case was studied in Appendix A in Ref. [15] but where we now must replace γ with γ^* . However, since $\gamma^* = \gamma$ to zero order in δu the results derived in Appendix A in Ref. [15] are still valid and we conclude that the effective medium theory result for σ_x and σ_y is exact to order δu^2 and that γ can be obtained from the matrix D involving only the surface roughness power spectrum.

6 The critical junction theory of fluid flow

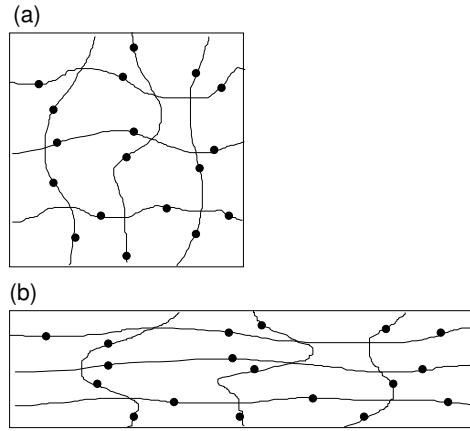


FIG. 5: (a) Percolating fluid flow channels (lines) and critical constrictions (black dots) for a $L \times L$ square unit system with isotropic roughness. (b) The percolating fluid flow channels and critical constrictions for a system obtained by stretching by a factor of 2 in the x -direction and $1/2$ in the y -direction (Pekeling number $\gamma = 4$). After this mapping, the concentration of flow channels is increased by a factor of 2 in the x -direction and reduced by a factor of $1/2$ in the y -direction. For a square unit $L \times L$ (not shown) the number of critical constrictions along each percolating flow channel is reduced by a factor of $1/2$ in the x -direction and increased by a factor of 2 in the y -direction. The net result is that the fluid flow conductivity is increased by a factor of 4 in the x -direction and reduced by a factor of $1/4$ in the y -direction, i.e., $\sigma_x = \gamma\sigma_0$ and $\sigma_y = \sigma_0/\gamma$, where σ_0 is the flow conductivity for the system with isotropic roughness in (a).

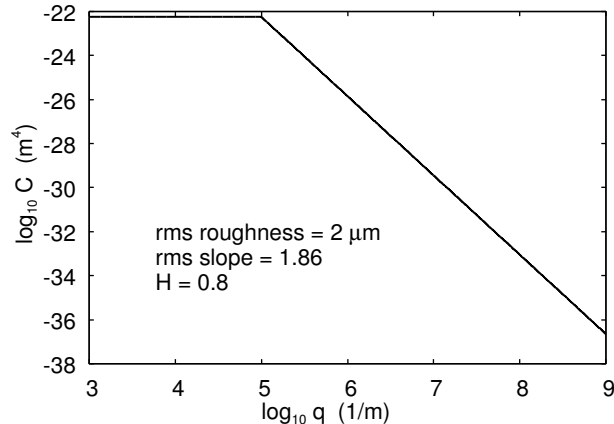


FIG. 6: Surface roughness power spectrum as a function of the wavenumber (log-log scale).

Consider a rubber seal. Assume first isotropic roughness and that the nominal contact region between the rubber and the hard counter-surface is a square area $L \times L$. We assume that a high-pressure fluid region occur for $x < 0$ and a low-pressure region for $x > L$. Now, let us study the contact between the two solids as we increase the magnification ζ . We define $\zeta = L/\lambda$, where λ is the resolution. We study how the apparent contact area (projected on the xy -plane), $A(\zeta)$, between the two solids depends on the magnification ζ . At the lowest magnification we cannot observe any surface roughness, and the contact between the solids appears to be complete i.e., $A(1) = A_0$. As we increase the magnification we will observe some interfacial roughness, and the (apparent) contact area will decrease. At high enough magnification, say $\zeta = \zeta_c$, a percolating path of non-contact area will be observed for the first time. We denote the most narrow constriction along this percolation path as the critical constriction. The critical constriction will have the lateral size $\lambda_c = L/\zeta_c$ and the surface separation at this point is denoted by u_c . We can calculate u_c using a recently developed contact mechanics theory[2]. As we continue to increase the magnification we will find more percolating channels between the surfaces, but these will have more narrow constrictions than the first channel which appears at $\zeta = \zeta_c$, and as a first approximation one may neglect the contribution to the leak rate from these channels. An accurate estimate of the leak rate is obtained by assuming that all the leakage occurs through the critical percolation channel, and that the whole pressure drop $\Delta P = P_a - P_b$ (where P_a and P_b is the pressure to the left and right of the seal) occurs over the critical constriction (of width and length $\lambda_c \approx L/\zeta_c$ and height u_c). We refer

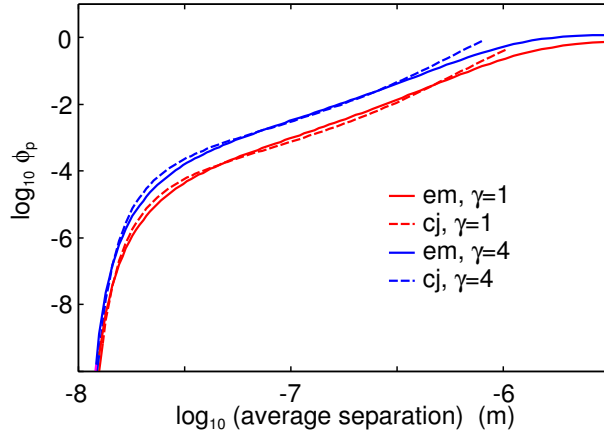


FIG. 7: Fluid pressure flow factor $\phi_p = 12\eta\sigma_x/\bar{u}^3$ as a function of the average surface separation \bar{u} (log-log scale). In the calculation we have used the surface roughness power spectra shown in Fig. 6 and the Young's elastic modulus $E = 10$ MPa. Results are shown for $\gamma = 1$ (red curves) and $\gamma = 4$ (blue curves) using the effective medium (em) theory (solid lines) and the critical junction (cj) theory (dashed curves).

to this theory as the critical-junction theory. If we approximate the critical constriction as a pore with rectangular cross-section (width and length λ_c and height $u_c \ll \lambda_c$), and if we assume an incompressible Newtonian fluid, the volume flow per unit time through the critical constriction will be given by (Poiseuille flow)

$$\dot{Q} = \frac{u_c^3}{12\eta} \Delta P \quad (37)$$

In deriving (37) we have assumed laminar flow and that $u_c \ll \lambda_c$, which is always satisfied in practice. The flow conductivity σ_{eff} can be obtained from \dot{Q} using $\dot{Q} = J_x L = \sigma_{\text{eff}}(\Delta P/L)L$ giving

$$\sigma_{\text{eff}} = \frac{u_c^3}{12\eta} \quad (38)$$

The following qualitative picture underpin the critical constriction model. At the critical magnification several fluid conducting channels may appear and each of them may have several critical constrictions as indicated in Fig. 5(a). Now when we perform the mapping indicated in Fig. 2, where we go from isotropic roughness in a square area $L \times L$ to the anisotropic roughness in a square area of the same size [dashed square in Fig. 2(c)], we increase the number of flow channels in the x -direction by a factor of $\gamma^{1/2}$, and on each flow channel we reduce the number of critical junctions by a factor of $\gamma^{-1/2}$. Hence the fluid conductivity $\sigma_x = \gamma\sigma_0$. In a similar way one can show that $\sigma_y = \sigma_0/\gamma$. Note that this imply $\sigma_x = \gamma^2\sigma_y$, which we derived above from the effective medium theory close to the contact area percolation threshold. Note that this agreement with the effective medium theory require that the fluid pressure drop over a critical constriction is not modified by the stretching-contraction of the system.

To illustrate the accuracy of the critical junction approach, In Fig. 7 I show the fluid pressure flow factor $\phi_p = 12\eta\sigma_x/\bar{u}^3$ as a function of the average surface separation \bar{u} (log-log scale). In the calculation we have used the surface roughness power spectra shown in Fig. 6 and the Young's elastic modulus $E = 10$ MPa. Results are shown for $\gamma = 1$ (red curves) and $\gamma = 4$ (blue curves) using the effective medium theory (solid lines) and the critical junction theory (dashed curves). As expected, the critical junction theory is accurate when the average surface separation is small enough but is inaccurate for very small contact pressures where the average surface separation is large; this is expected as for large average surface separation a nearly uniformly thick fluid film separate the surfaces and the fluid pressure drop will not occur over a small number of narrow constrictions, but will occur in nearly uniformly over the whole nominal contact area. However, this limiting case is not of interest in sealing applications.

7 Discussion

In Ref. [18] we used molecular dynamic simulations to study the percolation of the contact area with increasing pressure for Tripp numbers $0.5 < \gamma < 2$. We found that the results could be reasonably well fit with the formula $A/A_0 = \gamma/(1 + \gamma)$. However, the Bruggeman effective medium theory predict $A/A_0 = 0.5$ independent of γ , and it is clear from very simple arguments (see Sec. 2) that for an infinite system the percolation threshold does not depend

on the asymmetry (or stretching) parameter γ . Hence, the fact that the numerical simulations showed a dependency of A/A_0 on γ must be a finite-size effect.

Recently, Yang et al have performed a numerical study of the effect of surface roughness anisotropy on the percolation threshold of sealing surfaces[23]. For surfaces with isotropic roughness they found $A/A_0 \approx 0.48$, i.e., close to the effective medium theory prediction, and larger than the value 0.42 found by Dapp et al[26].

As γ increased from 0.5 to 1.66, Yang et al found that A/A_0 increased from 0.43 to 0.53, which is a weaker γ -dependency than given by $A/A_0 = \gamma/(1 + \gamma)$, which predicts that A/A_0 increases from 0.33 to 0.63. This result is expected since in the limit of an infinite system the percolation threshold is independent of γ , and for finite systems the γ -dependency must depend on the system size.

The good agreement found between the effective medium theory and the critical junction theory indicates that the basic picture behind the critical junction theory is accurate. The critical junction theory is based on the observation that when increasing the magnification, at high enough magnification, say $\zeta = \zeta_c$, a percolating path of non-contact area will be observed for the first time. As we continue to increase the magnification we find more percolating channels between the surfaces, but these will have more narrow constrictions than the first channel which appears at $\zeta = \zeta_c$, and as a first approximation one may neglect the contribution to the leak rate from these channels. This implies that the roughness observed when the magnification is increased beyond $\zeta = \zeta_c$ has a negligible influence on the leakage of a seal. In a recent comment, Papangelo et al[24] state that the leakage rate depends on the short distance cut-off length λ_1 (observed at the highest magnification ζ_1), which could be an atomic distance, but this is in general not the case unless the nominal pressure is so high as to move the critical constriction to the shortest length scale, which is nearly never the case in practical applications.

8 Summary and conclusion

I have studied the influence of anisotropic roughness on the fluid flow at the interface between two elastic solids. I have shown that for randomly rough surfaces with anisotropic roughness, the contact area percolates at the same relative contact area as for isotropic roughness, and that the Bruggeman effective medium theory and the critical junction theory gives nearly the same results for the fluid flow conductivity (and the fluid pressure flow factor). This shows (qualitatively) that, unless the nominal contact pressure is so high as to result in nearly complete contact, the surface roughness observed at high magnification is irrelevant for the fluid flow during squeeze-out, or for the leakage of stationary seals.

Acknowledgments: I thank M. Scaraggi for useful comments on the manuscript!

Appendix A: Two integrals

In Sec. 3 and 4 appeared two important integrals:

$$I_1 = \frac{1}{2\pi} \int_0^{2\pi} d\phi \frac{\cos^2 \phi}{\cos^2 \phi + \gamma^2 \sin^2 \phi} = \frac{1}{1 + \gamma} \quad (A1)$$

$$I_2 = \frac{1}{2\pi} \int_0^{2\pi} d\phi \frac{\sin^2 \phi}{\cos^2 \phi + \gamma^2 \sin^2 \phi} = \frac{1}{\gamma(1 + \gamma)} \quad (A2)$$

Note that $I_1 + \gamma^2 I_2 = 1$. The results above can be proved by integration in the complex plane: Introducing $z = e^{i\phi}$ and writing $\cos \phi = (z + 1/z)/2$ and $\sin \phi = (z - 1/z)/(2i)$ and performing the integration around the circle $|z| = 1$ result in the equations (A1) and (A2).

Appendix B: Flow current in elliptic insertion

The 2D fluid flow problem is mathematically similar to the electrostatic polarization of a dielectric material. Thus the fluid flow current and the electric current both satisfy $\nabla \cdot \mathbf{J} = 0$ (conservation of fluid volume and electric charge, respectively). The fluid current is related to the pressure gradient via $\mathbf{J} = -\sigma \nabla p$, where σ is the flow conductivity, and the electric current is related to the electric potential via $\mathbf{J} = -\sigma \nabla \phi$, where σ is the electric conductivity. Hence, results obtained in electrostatics for polarizable media can be used also for the fluid flow problem. In particular, from electrostatics it is known that if an elliptic region with constant dielectric properties is embedded in an infinite dielectric material with other dielectric properties, then the electric field (and hence the polarization) in the elliptic region will be constant, assuming that the electric field is constant far away from the elliptic region. The corresponding result for the fluid flow problem was used in Sec. 4.

Note that when σ is constant the equation $\nabla \cdot \mathbf{J} = 0$ gives $\nabla^2 p = 0$ (for fluid flow) and $\nabla^2 \phi = 0$ (for electrostatics). The results for the electric polarization problem for an elliptic insertion can be derived by solving the Laplace equation $\nabla^2 \phi = 0$ using elliptic coordinates[27] or by complex mapping methods[28].

-
- [1] C. Rotella, B.N.J. Persson, M. Scaraggi, P. Mangiagalli, *Lubricated sliding friction: Role of interfacial fluid slip and surface roughness*, The European Physical Journal E **43**, 9 (2020)
- [2] C. Yang and B.N.J. Persson, *Contact mechanics: contact area and interfacial separation from small contact to full contact*, J. Phys.: Condens. Matter **20**, 215214 (2008).
- [3] Martin H Müser, Wolf B Dapp, Romain Bugnicourt, Philippe Sainsot, Nicolas Lesaffre, Ton A Lubrecht, Bo NJ Persson, Kathryn Harris, Alexander Bennett, Kyle Schulze, Sean Rohde, Peter Ifju, W Gregory Sawyer, Thomas Angelini, Hossein Ashtari Esfahani, Mahmoud Kadkhodaei, Saleh Akbarzadeh, Jiunn-Jong Wu, Georg Vorlauffer, Andrs Vernes, Soheil Solhjoo, Antonis I Vakis, Robert L Jackson, Yang Xu, Jeffrey Streater, Amir Rostami, Daniele Dini, Simon Medina, Giuseppe Carbone, Francesco Bottiglione, Luciano Afferrante, Joseph Monti, Lars Pastewka, Mark O Robbins, James A Greenwood, *Meeting the contact-mechanics challenge*, Tribology Letters **65**, 118 (2017).
- [4] B.N.J. Persson, M. Scaraggi, *Lubricated sliding dynamics: flow factors and Stribeck curve*, The European Physical Journal E **34**, 1 (2011).
- [5] Patir Nadir, *Effect of surface roughness on partial film lubrication using average flow model based on numerical simulation*, University microfilms International, 300 North Zeeb Road, P.O. Box 1346.
- [6] N. Patir, H.S. Cheng, *An average flow model for determining effects of three-dimensional roughness on partial hydrodynamic lubrication*, J. Lubr. Technol. **100**, 12 (1978)
- [7] N. Patir, H.S. Cheng, *Application of average flow model to lubrication between rough sliding surfaces*, J. Lubr. Technol. **101**, 220 (1979).
- [8] F. Sahlin, A. Almqvist, R. Larsson, S.B. Glavatskih, *Rough surface flow factors in full film lubrication based on a homogenization technique*, Tribol. Int. **40**, 1025 (2007).
- [9] J.H. Tripp, *Surface roughness effects in hydrodynamic lubrication: The flow factor method*, J. Lubr. Technol. **105**, 458 (1983).
- [10] A. Almqvist, J. Fabricius, A. Spencer, P. Wall, *Similarities and differences between the flow factor method by Patir and Cheng and homogenization*, J. Tribol. **133**, xx (2011), doi:10.1115/1.4004078.
- [11] B.N.J. Persson, C. Yang, *Theory of the leak-rate of seals*, Journal of Physics: Condensed Matter **20**, 315011 (2008)
- [12] B. Lorenz, B.N.J. Persson, *Leak rate of seals: Effective-medium theory and comparison with experiment*, The European Physical Journal E **31**, 159 (2010).
- [13] B. Lorenz, B.N.J. Persson, *Time-dependent fluid squeeze-out between solids with rough surfaces*, The European Physical Journal E **32**, 281 (2010).
- [14] J. Peklenik, *New Developments in Surface Characterization and Measurement by Means of Random Process Analysis*, Proc. Inst. Mech. Eng. **182**, 108 (1967).
- [15] BNJ Persson, N Prodanov, BA Krick, N Rodriguez, N Mulakaluri, WG Sawyer, P Mangiagalli, *Elastic contact mechanics: Percolation of the contact area and fluid squeeze-out*, The European Physical Journal E **35**, 5 (2012).
- [16] L. Afferrante, F. Bottiglione, C. Putignano, B.N.J. Persson, G. Carbone, *Elastic contact mechanics of randomly rough surfaces: an assessment of advanced asperity models and Persson's theory*, Tribology Letters **66**, 75 (2018).
- [17] A. Almqvist, C. Campana, N. Prodanov, B.N.J. Persson, *Interfacial separation between elastic solids with randomly rough surfaces: comparison between theory and numerical techniques*, Journal of the Mechanics and Physics of Solids **59**, 2355 (2011).
- [18] B.N.J. Persson, *Fluid dynamics at the interface between contacting elastic solids with randomly rough surfaces*, Journal of physics: Condensed matter **22**, 265004 (2010)
- [19] D.A.G. Bruggeman, *Berechnung verschiedener physikalischer Konstanten von heterogenen Substanzen*, Ann. Physik (Leipzig) **24**, 636 (1935).
- [20] P.A. Fokker, *General Anisotropic Effective Medium Theory for Effective Permeability of Heterogeneous Reservoirs*, Transport in Porous Media **44**, 205 (2001).
- [21] M. Scaraggi, *Lubrication of textured surfaces: A general theory for flow and shear stress factors*, Physical Review E **86**, 026314 (2012)
- [22] M. Scaraggi, *The friction of sliding wet textured surfaces: the Bruggeman effective medium approach revisited*, Proceedings of the Royal Society A: Mathematical, Physical and Engineering Sciences **471**, 20140739 (2015).
- [23] Z. Yang, J. Liu, X. Ding and F. Zhang, *The Effect of Anisotropy on the Percolation Threshold of Sealing Surfaces*, J. Tribol. **141**, 022203 (2019).
- [24] A. Papangelo and M. Ciavarella, *Comments on the percolation threshold of sealing surfaces and Persson's theory*, J. Tribol. January (2020).
- [25] Z. Yang, J. Liu, X. Ding and F. Zhang, *Reply to comments on the percolation threshold of sealing surfaces and Persson's theory*, J. Tribol., Paper No: TRIB-19-1544 <https://doi.org/10.1115/1.4046134> Published Online: January 27, 2020
- [26] W.B. Dapp, A. Lücke, B.N.J. Persson, and M.H. Müser *Self-Affine Elastic Contacts: Percolation and Leakage*, Phys. Rev. Lett. **108**, 244301 (2012)

- [27] P.M. Morse and H. Feshbach, *Methods of Theoretical Physics*, Part 2, page 1199, McGraw Hill (1953).
- [28] P.J. Olver, *Complex Analysis and Conformal Mapping*,